Journal of Inflammation Research

Dovepress
Taylor & Francis Group

Open Access Full Text Article

ORIGINAL RESEARCH

Bioinformatics and Network Pharmacology Identify the Therapeutic Role of Guominkang in Allergic Asthma by Inhibiting PI3K/Akt Signaling

Honglei Zhang[1,2,*], Haiyun Zhang[1–3,*], Lei Wang[4], Yihang Zhang[1,2], Linhan Hu[1,2], Juntong Liu[1,2], Yumei Zhou[1], Ji Wang[1]

[1]National Institute of TCM Body Constitution and Preventive Medicine, Beijing University of Chinese Medicine, Beijing, 100029, People's Republic of China; [2]College of Traditional Chinese Medicine, Beijing University of Chinese Medicine, Beijing, 100029, People's Republic of China; [3]Dalian Women and Children's Medical Group, Dalian, 116000, People's Republic of China; [4]Hubei Shizhen Laboratory, Hubei University of Chinese Medicine, Wuhan, Hubei, 430065, People's Republic of China

*These authors contributed equally to this work

Correspondence: Yumei Zhou; Ji Wang, National Institute of TCM body constitution and Preventive Medicine, Beijing University of Chinese Medicine, Beijing, 100029, People's Republic of China, Email ymzhou666@163.com; doctorwang2009@126.com

Background: As a classical regulating formula, Guominkang (GMK) has been extensively employed in clinical practice to treat the allergic asthma (AA) and alleviate allergy symptoms, however, the underlying mechanism remains elusive. The aim of this study was to explored the mechanism of action through which GMK combats AA.

Methods: Potential target genes for the compounds were identified from the database and subjected to functional enrichment analysis. Subsequently, a protein-protein interaction (PPI) network was constructed in order to screen the core target and confirmed by molecular docking. An asthma model was further developed in mice and airway hyperresponsiveness and lung pathological changes were observed following drug administration. The expression of PI3K and AKT proteins in lung tissues was then detected by Western blotting. Subsequently, the GSE104468 data were normalised and visualised using the R language, compared to the PI3K-Akt pathway gene set to identify overlapping genes, constructed a PPI network and analysed correlations between genes.

Results: 267 compounds and 475 disease-relevant GMK targets have been obtained, primarily in the areas of chemokine binding, drug binding, and PI3K-Akt pathway modulation. Molecular docking simulations revealed that predicted targets (PI3K, TNF, IL6, AKT1, SRC, TP53, and STAT3) could be closely bonded with component of GMK. According to in vivo experiments, GMK could reduce mucus obstruction and airway inflammation ($P < 0.05$), decrease airway hyperresponsiveness ($P < 0.05$), and inhibited the PI3K-Akt pathway ($P < 0.05$). After normalising the genes in the dataset between AA and healthy individuals, GO showed that 388 DEGs were associated with PI3K/AKT signaling pathway. The PPI network showed that the overlapping gene were located in the centre of asthma-associated network and that exhibited a correlation with the PI3K-Akt signaling pathway.

Conclusion: Based on our findings, GMK potentially acts via the PI3K/Akt pathway and alleviates allergic symptoms in AA.

Keywords: allergic diseases, traditional Chinese medicine, network pharmacology, PI3K/Akt signaling pathway

Introduction

Allergic asthma (AA) is the result of heterogeneous, complex gene-environment interactions involving multiple cells, especially mast cells, eosinophils and T-lymphocytes, in chronic airway inflammation with different clinical phenotypes, inflammation and remodelling. In susceptible individuals, this inflammation can cause recurrent episodes. The most common symptoms of AA include wheezing, shortness of breath, chest tightness and/or coughing, which are often present at night and/or in the early hours of the morning. Additionally, individuals with AA tend to have increased airway responsiveness to a wide range of irritants. AA affects between 1–18% of the global population,[1] with an estimated 339 million people suffering from the condition, resulting in 1000 deaths per day, as reported in the 2018 Global Asthma

Received: 26 June 2024
Accepted: 21 December 2024
Published: 25 February 2025

Report.[2] The current clinical treatments for this disease only control the symptoms and reduce inflammation. For example, the most commonly used biologics globally are anti-IgE monoclonal antibodies, which account for 78% of all treatments, followed by anti-interleukin (IL)-5 antibodies (43.9%), anti-IL-13R/IL-4R antibodies (36.7%), and anti-IL-5R antibodies (26.7%).[3] The reported adverse reactions include local reactions at the injection site (74%), followed by allergic reactions (6.8%), delayed rashes (5.1%), and serious cutaneous adverse reactions.[4] This causes a lot of inconvenience to the patient's life and work. In addition, corticosteroids are one of the main pharmacological treatments for asthma with anti-inflammatory properties, and according to a meta-analysis by Bateman et al (64 RCTs, 42,527 patients), an inhaled corticosteroid (ICS) regimen was found to improve patients' quality of life, and the inhaled corticosteroid + long-acting β2-agonist fixed-dose combination was well tolerated and safe, and current clinical guidelines recommend prescribing a combination of the two for treatment.[5]

With progressive development over millennia, traditional Chinese medicine (TCM) have gained widespread acceptance in treating numerous illnesses, including allergic diseases. The herbal formulation Guominkang (GMK) formula was found to be markedly effective in regulating allergic diseases, including allergic rhinitis, AA, and atopic dermatitis.[6] Previously, we have reported that GMK can suppress the recruitment of inflammatory cells, reduce mucus production, decrease airway resistance, attenuate allergic symptoms in asthmatic mouse models, and reestablish the cytoimmune homeostasis of Th1/2 and regulatory T cells (Tregs)/Th17 cells.[7] Accordingly, it can be speculated that GMK may inhibit AA progression by regulating several targets and pathways. Currently, the effect of TCM on diseases is being explored mainly by overlapping interactions between components and disease targets to unravel the underlying mechanisms of TCM therapy.

PI3K/Akt is a typical signal transduction pathway that regulates a number of cellular processes, including cell growth, proliferation, motility, metabolism and survival and plays a crucial role in the pathogenesis of allergic diseases. The PI3K/AKT pathway is a key contributor to allergic airway inflammation, promoting eosinophil recruitment and Th1/Th2 immune imbalance.[8] The specific PI3K inhibitor Ly294002 has been demonstrated to effectively attenuate airway inflammation, airway remodelling and eosinophil infiltration in asthma mice.[9] Consequently, numerous herbs and herbal extracts were observed to alleviate inflammation and lung injury in the OVA-LPS-induced AA mouse model, with the PI3K signaling pathway playing a pivotal role.[10,11]

This study employed network pharmacology, molecular docking, experimental methods and bioinformatics to analyze the key components and targets of GMK that exert therapeutic effects on AA, as well as the signaling pathways of action. We carried out preliminary validation through animal experiments, which provided a reference for the precise therapeutic targets of GMK and the multi-targets for the treatment of AA. The workflow is presented as a graphical summary (Figure 1).

Materials and Methods

Data Source and DEG in Asthma

The Asthma-related microarray datasets GSE104468 were downloaded from the Gene Expression Omnibus (GEO) database (https://www.ncbi.nlm.nih.gov/geo/). The microarray GSE104468, detected by GPL21185, Included 24 nasal samples from 12 asthma patients and 12 healthy samples. The PI3K-Akt related genes were obtained from the KEGG database, which contains 359 genes (KEGG PATHWAY: hsa04151). Raw data were batch corrected to remove batch effects for further analysis. Differentially expressed genes (DEGs) were screened by using the "limma" package with $P < 0.05$ and $|\log FC| > 0.9$ indicating statistically significant differences.[12],388 genes were analysed further. The R language programs "heatmap" and "ggplot2" were used to create heat maps, volcano maps and box line plots.

Analyses of DEGs Function

To investigate the function of the DEGs in asthma, a consensus clustering algorithm was employed to evaluate the optimal cluster numbers and robustness. The R package "ConsensusClusterPlus" implemented the above steps for 1000 iterations to guarantee the robustness of classification. Gene set enrichment analysis (GSEA) was performed on the gene expression matrix by applying the "clusterProfiler" package. The "ggplot2" packages were used to perform Gene

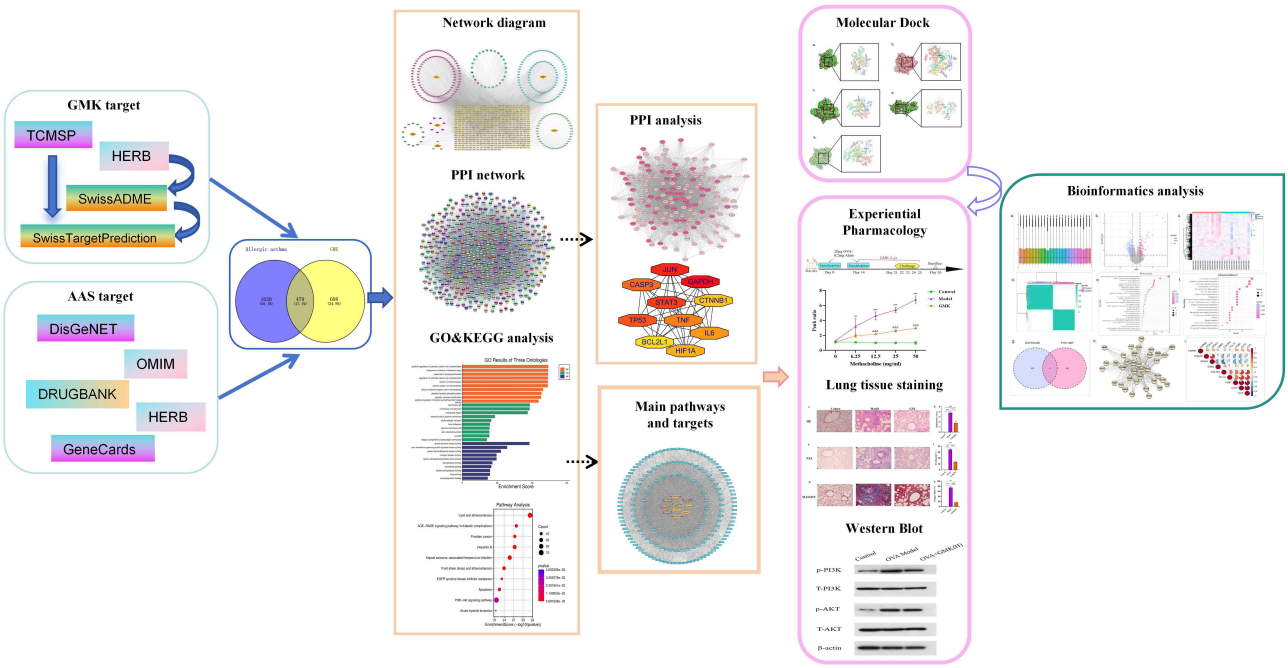

Figure 1 Flow chart of this study.

Ontology (GO) and Kyoto Encyclopedia of Genes and Genomes (KEGG) enrichment analyses on DEGs. The "ggvenn" package was used to depict the intersecting genes of the dataset differential genes and signaling pathways. The "corrplot" and "paletteer" packages were used to profile the heatmap of the correlation coefficients of the intersecting genes.

Screening of Active Ingredients of GMK

The six GMK components were entered into the Traditional Chinese Medicine Systems Pharmacology Database and Analysis Platform (TCMSP, https://old.tcmsp-e.com/tcmsp.php) and the HERB (http://herb.ac.cn/) databases to determine the chemical composition of the herbal medicines, with descending screening conditions in the TCMSP website set as follow: oral bioavailability (OB) ≥ 30 and drug-likeness (DL) ≥ 0.18.[13,14] The pharmacochemical components of HERB were downloaded from PubChem (https://pubchem.ncbi.nlm.nih.gov/) with Canonical SMILES for each component. These active ingredients were screened using pharmacokinetic parameters from the swissADME (http://www.swissadme.ch/) database, using the criteria gastrointestinal absorption (GI) = High and the rule of five (Lipiskin, Ghose filter, Veber filter, Egan filter, and Muegge filter) presenting "yes" ≥ 2 to comply with ADME (absorption, distribution, metabolism, and excretion) characteristics of the drug and demonstrate that the orally administered drug can be absorbed.[15,16]

Target Prediction of Active Ingredients of GMK

The Canonical SMILES of each component obtained by database screening were uploaded to SwissTargetPrediction (http://www.swisstargetprediction.ch/) to establish a list of targets for each active component, proteins with the probability > 0 were considered more biologically active targets. To obtain uniform gene names, the UniProt (http://www.uniprot.org) website was used to perform ID conversion, download the reviewed files converted to uniform Homo sapiens, and obtain the UniProt IDs of all targets.[17,18]

Collection of Disease-Related Targets for AA

The disease name "allergic asthma" was entered into the disease search field of the following five databases: OMIM (https://omim.org/),[19] DisGeNET (https://www.disgenet.org/),[20] GeneCards (https://www.genecards.org/),[21] HERB

https://doi.org/10.2147/JIR.S484251

(http://herb.ac.cn/), Drugbank (https://www.drugbank.ca/),[22] the relevant targets of the disease were collected and downloaded from each database. Finally, the UniProt ID and human gene name were obtained from the UniProt database.

Compounds-Disease-Targets Network Construction

The predicted targets of each component (obtained from the above steps in each database) were uploaded to the Venn online tool with AA-related targets. Subsequently, common target sets of drugs and diseases were compared to obtain an intersection set as the GMK target for treating AA. The Cytoscape 3.9.0 software was employed to generate tables for the purpose of a visual analysis of compounds-disease-targets networks.[23]

Protein-Protein Interaction, PPI

PPI networks, connected by protein interactions, can systematically analyze massive protein interactions in biosystems and are critical to explore molecular mechanisms of bio-signaling and energetic substance metabolism in physiological and pathological states, as well as to clarify functional linkages among proteins. The target genes in the above intersection were uploaded to the STRING database (https://string-db.org/), and species-selected Homosapiens and PPI network relationships were obtained using the default parameters of the system. To obtain the core target networks, the CytoNCA plugin wasused to calculate topological parameters in PPI networks and perform an in-depth analysis of the properties of nodes in interactive networks. The top 10 key genes were calculated using cytoHubba, with color shades representing the keyness of genes.[24–26]

Enrichment Analysis

Enrichment categories and extent of target genes in GO and KEGG were analyzed. GO analysis included molecular function (MF), cellular component (CC), and biological processes (BP). The R (3.6.3) ggplot2 package with the clusterProfiler package and KOBAS (http://kobas.cbi.pku.edu.cn/) website were used with the screening criteria set at $P < 0.05$.

Molecular Docking

First, candidate proteins were entered into the UniProt website, and structures with a recent update date and high resolution were selected and linked to the PDB website for download. The selected small-molecule ligand 3D structures were downloaded from the PubChem website, and proteins and small molecules were processed using the AutoDock Tools software and output in their respective pdbqt format files.

Animal Model and GMK Preparation

BALB/c mice (6-8-week-old) were purchased from Beijing Vital River Laboratory Animal Technology Co. and housed in a specific pathogen free (SPF) environment. All animal experiments followed the standards of the Animal Care and Use Committee of the Beijing University of Chinese Medicine, AAALAC and IACUC guidelines.

Mice were randomly divided into three groups, with 12 animals assigned per group: the blank control group (control), model group (model), and GMK treatment group (GMK). The AA model was established as described in our previous study.[7] Sensitization phase: On day 0 and day 14, respectively, each mouse was intraperitoneally administered 0.2 mL of ovalbumin (OVA) antigen solution containing 20 μg OVA (Cat#A5503, Sigma-Aldrich, USA) and 0.2 mg aluminum adjuvant (Cat#77161, Invitrogen, USA), mice in the blank group were intraperitoneally administered the same volume of saline containing 0.2 mg aluminum adjuvant. Stimulation phase: From day 21 to day 25, at least 30 min before completing administration, mice were nebulized with 1% OVA saline solution for 30 min, the blank group was nebulized with the same volume of phosphate-buffered saline (PBS) for 30 min.

The GMK formula was as follows: Wu-Mei (Mume Fructus), Shou Wu Teng (Polygoni Multiflori Caulis), Ling Zhi (Ganoderma), Fang Feng (Saposhnikoviae radix), Chan Tui (Cicadae Periostracum), Tian Ma (Gastrodiae Rhizoma), these components were purchased and immersed in deionized water for 30 minutes, and then decocted them at 100°C. The same volume of deionised water was added again with the same conditions of decoction and repeated once more. 19.5 g/kg of GMK was administered once daily by gavage from day 14 to day 25.

Airway Methacholine (Mch) Excitation Assay in Mice

Acetylcholine powder was dissolved in PBS to achieve gradient concentrations of 0, 6.25, 12.5, 25, and 50 mg/mL, and each mouse was stimulated for 5 min. Enhanced pause (Penh) values of each group of mice stimulated with different acetylcholine concentrations were measured noninvasively. On experiment completion, the Penh values of the mice in each group were counted and calculated, and finally expressed as Penh ratio. The calculation formula is: the average value of Penh in the 5-minute interval of methacholine/the average value of Penh in the 5-minute interval of PBS stimulation.

Pathological Tissue Staining

Lung tissues were fixed in 4% paraformaldehyde solution for 24 h and then subjected to HE staining, PAS staining and Masson staining (Wuhan Servicebio Technology CO.,LTD, China). The sections were dehydrated with 50%, 70%, 80%, 95% ethanol and anhydrous ethanol in turn, and then dipped in xylene for several hours after being transparent, embedded in regular paraffin wax, and stored in slices. HE staining: paraffin sections were dewaxed, stained with hematoxylin-eosin, and dehydrated and sealed, and the nuclei of the cells appeared to be blue to blue-purple and the cytoplasm of the cells appeared to be red under the microscope. PAS staining: the sections were dewaxed and acidified with periodic acid, washed in water, stained with chevron, and sealed with dehydration, and the mucus material appeared to be purple-red. Masson staining: paraffin sections were sequentially deparaffinised, stained with potassium dichromate, stained with ferric hematoxylin, stained with magenta, stained with phosphomolybdic acid, stained with aniline blue and sealed, and the local histopathological changes were observed under the microscope.

Western Blotting

Total protein was extracted from the RIPA lysate and quantified by the BCA method. Subsequently, protein separation was achieved by 8% sodium dodecyl sulfate-polyacrylamide gel electrophoresis, carefully place the membrane in a film transfer clip, and activate the polyvinylidene difluoride (PVDF) membrane in methanol, followed by transfer to PVDF membranes in TBST buffer. The membranes were blocked using PBST containing 5% skim milk powder at 37°C for 2 h. The primary antibodies (Akt (56 kDa, Abcam, ab238477, 1:1000), P-AKT (56 kDa, Abcam, ab81283, 1:1000), PI3K (123 kDa, Abcam, ab151549, 1:1000), p-PI3K (84 kDa, Abcam, ab182651, 1:1000), β-actin (42 kDa, Abcam, ab8227, 1:1000)) were incubated at 4°C overnight. Incubate the secondary antibody for one hour at room temperature. The bands on PVDF membrane were detected using chemiluminescent substrates and quantified density using the Image Lab 5.2 software. All experiments were performed in triplicate.

Statistical Analysis

SPSS 26.0 software was used to analyze the data. The experimental results were obtained from three independent replications. All data were tested for normality and chi-square. Each group's results are expressed as mean ± SEM. Differences between the groups were analyzed using unpaired t-tests or chi-square tests, depending on the type of data, while one-way or multi-way ANOVA was utilised for multiple group comparisons. The statistically significant difference is indicated by P value < 0.05. GraphPad Prism 9.5.0 software was used to draw statistical charts.

Results

Active Compounds of GMK

Searching the TCMSP and HERB databases, we identified the following active compounds: Ganoderma, Saposhnikoviae radix, Mume Fructus, Cicadae Periostracum, Caulis Polygoni Multiflori, and Gastrodiae Rhizoma, of these, the pharmacologically active ingredients were screened using the rule of five. After eliminating compounds without relevant targets and duplicate data, 50 compounds of Mume Fructus (Wu-Mei), 4 of Polygoni Multiflori Caulis (Shou Wu Teng), 115 of Saposhnikoviae radix (Fang-Feng), 128 of Ganoderma (Ling Zhi), 17 of Gastrodiae Rhizoma (Tian Ma), and 10 of Cicadae Periostracum (Chan Tui) were identified, among which 27 overlapping ingredients were named using their PubChem IDs in the network. Overall, 267 compounds were obtained, with 1177 related targets predicted. Table 1 presents information regarding the top ten compounds.

Table 1 Top 10 Compounds in the Ingredient-Target Network of GMK

PubChem CID	Compound Name	Molecular Formula	Degree	Average Shortest Path Length	Betweenness Centrality	Closeness Centrality
21633085	Methyl lucidenate F	C28H38O6	179	2.515503876	0.014089733	0.397534669
11271456	Methyl lucidenate Q	C28H42O6	163	2.525839793	0.006498187	0.395907928
21,635716	15alpha,26-Dihydroxy-5alpha-lanosta -7,9(11),24-triene-3-one	C30H46O3	149	2.53875969	0.008205865	0.39389313
73400	Dauricine	C38H44N2O6	116	2.611111111	0.015706075	0.382978723
442126	Decursin	C19H20O5	115	2.549095607	0.011638645	0.392295996
14015434	Epoxyganoderiol A	C30H48O4	115	2.546511628	0.007910494	0.392694064
21636089	Methyl lucidenate A	C28H40O6	115	2.53875969	0.007471263	0.39389313
132,113	3,7,12,23-Tetrahydroxy-26,28-epoxy-16,23-cyclolanost-8-ene-11,15,26-trione	C30H42O8	113	2.481912145	0.014611507	0.402915148
643684	Ricinoleic acid	C18H34O3	113	2.57751938	0.008031063	0.387969925
10212	Imperatorin	C16H14O4	111	2.598191214	0.007354542	0.384883143

Construction of a Drug-Compound-Target Network

The keyword "allergic asthma" was used to search and download each database separately, and 2109 disease targets were obtained after eliminating duplicate data. The targets of each component and disease were entered into the Venn mapping website to obtain the intersection and plot the Venn diagram (Figure 2a). The plotted Venn diagram revealed 479 genes in the central intersection, and 475 were obtained after converting UniProt ID to the gene name, which showed that one-quarter of the GMK targets were disease-related genes. The rhombus represents the drug, the oval represents the compound, the circle represents the compound with overlapping related drugs, the color corresponds to different compounds, and the round rectangle represents the target. The drug-compound-target network graph includes 775 nodes and 11,138 edges (Figure 2b).

PPI Network and Freedom Analysis With Screening of Hub Genes

Files regarding the interaction relationship obtained from the STRING database were imported into Cytoscape 3.9.0 for visualization (Figure 2c). CytoNCA screened core targets based on centrality analysis, with proteins associated with the PI3K-Akt pathway indicated in dark pink (Figure 2d). Among them, the top 10 nodes in terms of degree were TNF, IL6, AKT1, ALB, GAPDH, IL1β, SRC, TP53, VEGFA, and STAT3 (see Table 2 for node details). In the cluster analysis, there were seven modules with MCODE scores ≥ 5 (see Table 3 for module details).

The following ten common target hub genes were identified according to the default MCC algorithm in the cytoHubba plugin, with degree values in descending order and indicated in dark to light colors. The top ten hub genes were GAPDH, JUN, STAT3, TP53, CASP3, TNF, IL-6, HIF1A, CTNNB1, and BCL2L1 (Figure 2e).

GO Functional Enrichment and KEGG Pathway Analysis

The results presented entries with gene enrichment *P*.adj ≤ 0.05: BP mainly involved processes such as response to molecule of bacterial origin, response to lipopolysaccharide, CC mainly involved processes such as membrane raft, membrane microdomain, and external side of plasma membrane, MF mainly involved processes such as chemokine binding, protein tyrosine kinase activity and drug binding (Figure 3a-c). Significant pathways are shown in the bubble diagram, where predominant signaling pathways include the PI3K/Akt signaling pathway and apoptosis (Figure 3d). Accordingly, the effects of GMK on AA appear to be mediated through multiple compounds, targets, and pathways.

The top 10 signaling pathways with the smallest P values were visualised using Cytoscape 3.9.0, along with their corresponding targets. Consequently, a network graph comprising 178 nodes and 4719 edges was generated (Figure 3e). Using the Network Analysis tool, the average degree of signaling pathway nodes was 53.02, with 74 nodes exceeding this value. The main signaling pathways and target information are listed in Tables 4 and 5, respectively.

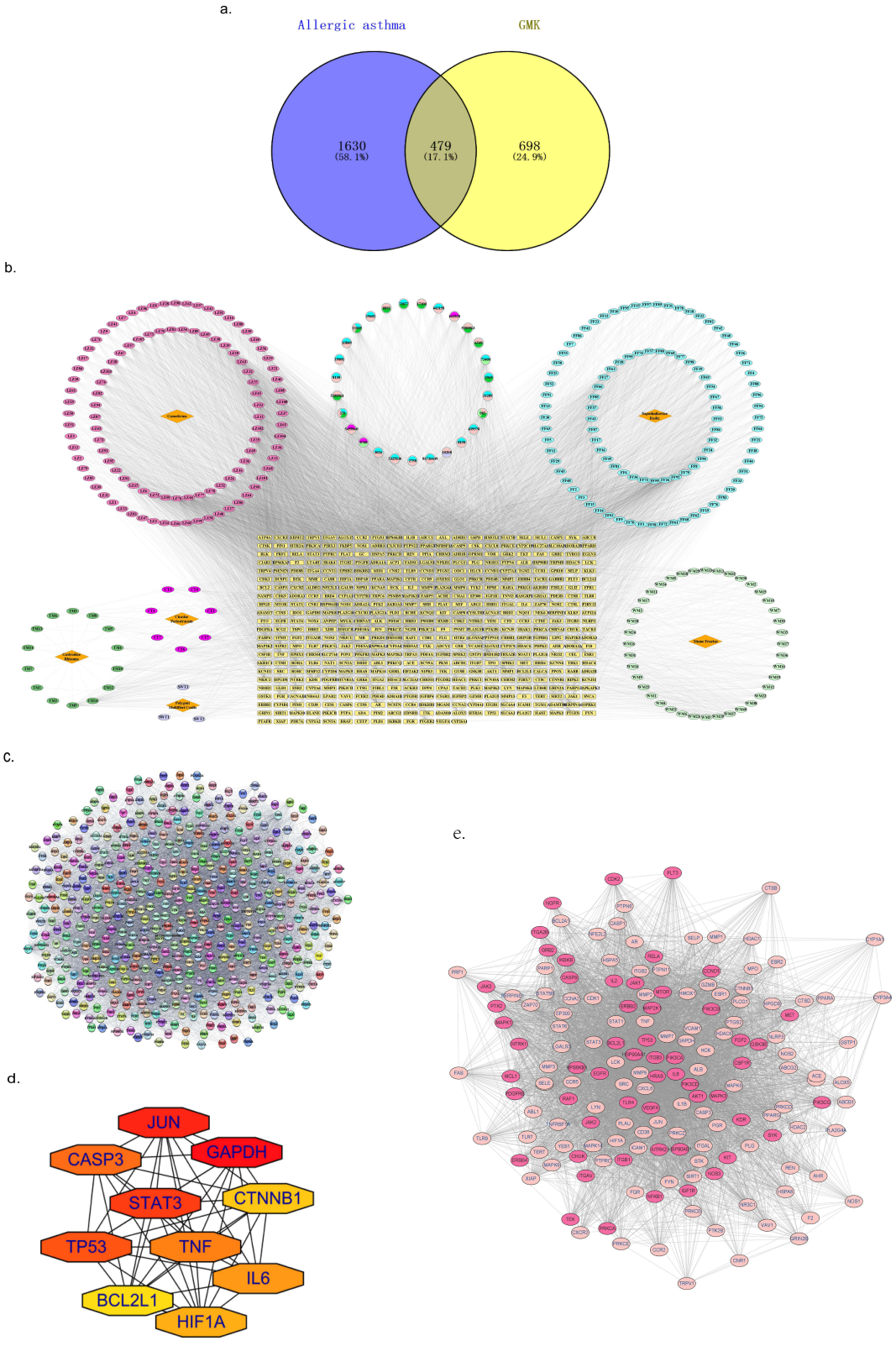

Figure 2 Network pharmacological analysis. (**a**) Venn diagram of active ingredients and disease targets (**b**)Network of Compounds-disease-targets (**c**) PPI network of common targets of GMK and AA (472 nodes,10735 edges) (**d**) cytoNCA PPI network (164 nodes,5383 edges) (**e**) Hub gene of PPI network.

https://doi.org/10.2147/JIR.S484251

Table 2 Top 10 Targets in Protein-Protein Interaction Network of GMK and AR

Name	Degree	Betweenness	Closeness
TNF	271	14,324.56835	0.700892857
IL6	256	11,618.75234	0.68558952
AKT1	250	10,935.69757	0.678674352
ALB	231	12,369.2706	0.658741259
GAPDH	226	7931.796718	0.650552486
IL1β	210	5521.055232	0.639945652
SRC	205	6302.487251	0.629679144
TP53	192	4296.922783	0.61892247
VEGFA	190	3664.970737	0.618110236
STAT3	189	3623.107228	0.60931436

Table 3 Modules of the Protein-Protein Interaction Network of Common Targets of GMK and AR

NO	Targets	MCODE Score	Nodes	Edges
Cluster 1	CCND1, MET, NOS2, KDR, NFE2L2, TP53, SIRT1, EP300, ESR2, JUN, MTOR, HSPA5, MMP7, JAK2, SRC, MAPK1, PTGS2, ALB, CXCL8, ESR1, PTK2, PTPRC, CTNNB1, IL2, BCL2L1, PLG, MMP2, HRAS, HSP90AA1, GAPDH, AKT1, ERBB2, MCL1, EGFR, STAT3, MAPK8, AR, IKBKB, STAT1, CASP1, PPARG, MAPK14, MMP9, GSK3B, TLR4, NR3C1, FGF2, TNF, MAPK3, IL1B, PPARA, CASP8, STAT5B, PGR, MAP2K1, CASP3, HDAC1, IL6, CASP9, RELA, IGF1R, PARP1, TNFRSF1A, HMOX1, HIF1A, VEGFA, XIAP	52.242	67	1724
Cluster 2	REN, AXL, GRB2, PLCG1, NOS3, KIT, CCR2, CDK1, FLT3, ITGB1, FYN, PDGFRA, NOX4, MMP1, ERBB4, ICAM1, PIK3CA, ABL1, ACE, RPS6KB1, MMP13, PLAU, JAK3, SERPINE1, NTRK1, JAK1, LYN, ARG1, CCNA2, CDK2, PRKCD, PDGFRB, LGALS3, ALK, DUSP1, ABCB1, LCK, MMP3, NFKB1, HPGDS, AHR, PRKCA, HSPA8, PTPN11, CHUK, FAS, SELE, SHH, NLRP3, MAPK9, VCAM1, RAF1, TERT, STAT6	13.774	54	365
Cluster 3	PTPN6, PLAT, PIK3CG, PIK3CB, GSR, PRF1, BTK, ITGB3, HSP90B1, ELANE, HDAC4, TBK1, MMP8, HSP90AB1, HCK, SYK, CCR5, YES1, CSK, CSF1R, F3, MAP2K2, PRKCZ, PKM, TLR9, PTK2B, CXCR2, SPHK1, HDAC6, TEK, GZMB, SELP, TGFBR1, TYK2, BCL2A1, IRAK1, VAV1, MPO, HDAC2, IRAK4, TLR7, ZAP70, TGFBR2, MAP3K5, SIRT2, VDR	7.244	45	163
Cluster 4	P2RX3, SCN10A, SCN9A, TRPM8, TRPV4	5	5	10

Molecular Docking Verification

The top 10 PPI and targets of the main pathway-target network were identified, along with the key targets PI3K. These were then molecularly docked with the top 10 compounds using AutoDock Vina software. The crystal structures of the 7 targets with higher resolution were downloaded: PI3K (PDB ID:5JHB), TNF (PDB ID:4Y6O), IL6 (PDB ID:1ALU), AKT1 (PDB ID:1UNQ), SRC (PDB ID:7NG7), and TP53 (PDB ID:2VUK), and STAT3 (PDB ID:6NJS). The chemical structure SDF files of each compound were downloaded from the PubChem database (Table 6), and the docking fraction between compound-target was less than −5 kcal/mol, indicating that the corresponding compound and target had a higher binding affinity (Table 7), and the binding positions and sites for the five pairs of composite target interactions are shown in results (Figure 3f-j).

GMK Inhibits PI3K/Akt Signaling Pathway Activity in AA Mice

The AA animal model was constructed using the classical OVA method (Figure 4a). From the Penh results of each group of mice, GMK can be known to attenuate the airway resistance in AA mice (Figure 4b). Compared with mice in the control group, mice in the model group showed an increasing trend in the Penh ratio when stimulated with 0, 6.25, 12.5, 25, and 50 mg/mL acetylcholine ($P < 0.01$), thereby corroborating the modelling of AA mice, the GMK group had lower Penh

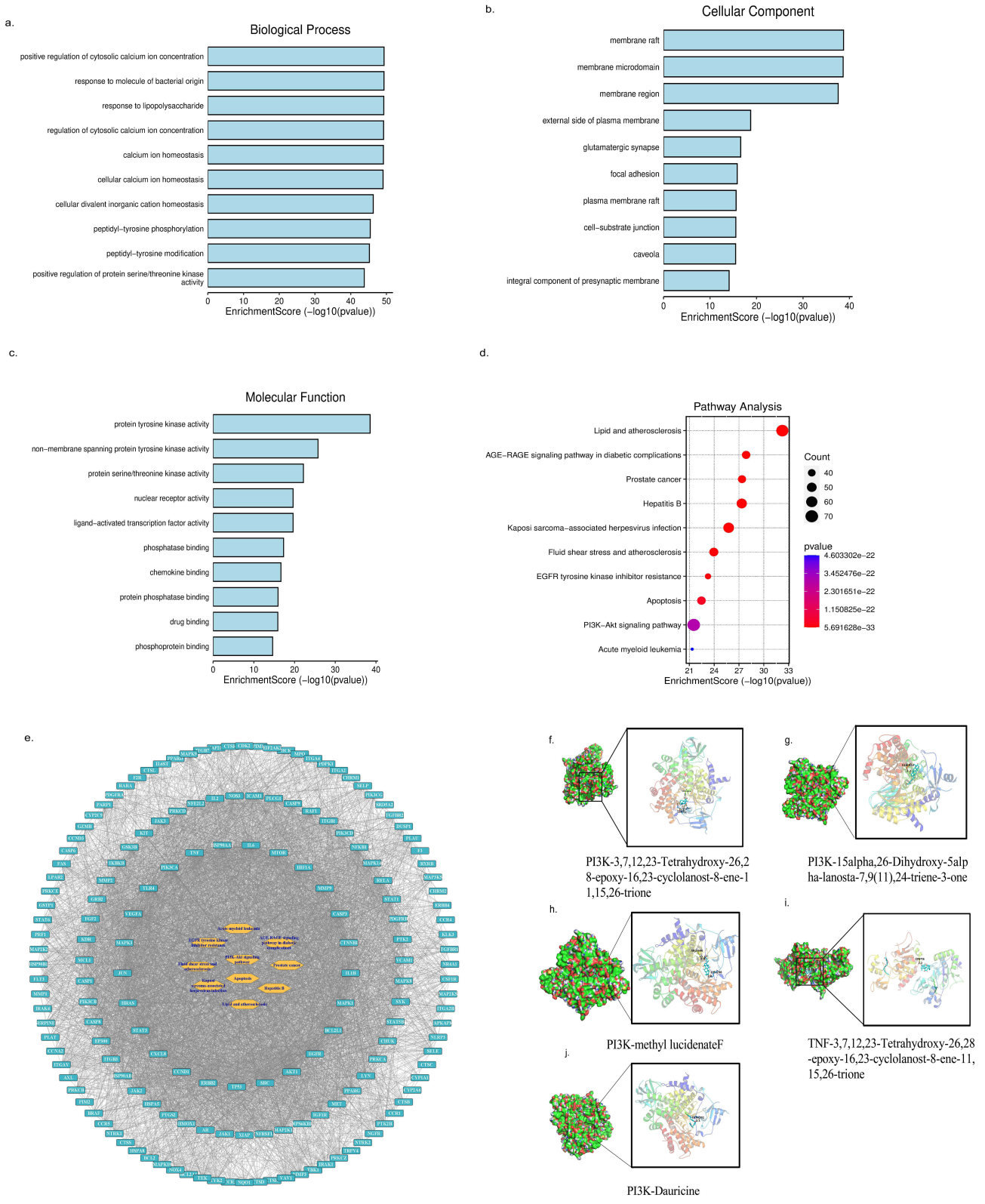

Figure 3 Functional analysis of the target. (**a-c**) GO functional and (**d**) KEGG pathway enrichment analysis (**e**) Network of the main pathways and targets (178 nodes,4719 edges) (**f**) PI3K-3,7,12,23-Tetrahydroxy-26,28-epoxy-16,23-cyclolanost-8-ene-11,15,26-trione (132113) Dock (**g**) PI3K-15alpha,26-Dihydroxy-5alpha-lanosta-7,9(11),24-triene-3-one (21635716) Dock (**h**) PI3K-methyl lucidenateF (21633085) Dock (**i**) TNF-3,7,12,23-Tetrahydroxy-26,28-epoxy-16,23-cyclolanost-8-ene-11,15,26-trione (132113) Dock (**j**) PI3K-Dauricine (73400) Dock.

https://doi.org/10.2147/JIR.S484251

Table 4 KEGG Pathways of Main Pathway-Target Network of GMK Treatment for AR (Top 10)

Name	Degree	Average Shortest Path Length	Betweenness Centrality	Closeness Centrality	Clustering Coefficient
PI3K-Akt signaling pathway	69	1.627118644	0.010938049	0.614583333	0.445865303
Lipid and atherosclerosis	66	1.632768362	0.010634473	0.612456747	0.491375291
Kaposi sarcoma-associated herpesvirus infection	56	1.694915254	0.004366174	0.59	0.555194805
Hepatitis B	53	1.717514124	0.002121369	0.582236842	0.554426705
Fluid shear stress and atherosclerosis	46	1.751412429	0.003230538	0.570967742	0.468599034
Apoptosis	44	1.785310734	0.004066625	0.560126582	0.477801268
AGE-RAGE signaling pathway in diabetic complications	43	1.779661017	0.001662977	0.561904762	0.568106312
Prostate cancer	42	1.774011299	0.004409695	0.563694268	0.527293844
EGFR tyrosine kinase inhibitor resistance	35	1.81920904	0.000438	0.549689441	0.72605042
Acute myeloid leukemia	31	1.870056497	0.001512914	0.534743202	0.464516129

Table 5 Targets of Main Pathway-Target Network of GMK Treatment for AR (Top 10)

Name	Degree	Average Shortest Path Length	Betweenness Centrality	Closeness Centrality	Clustering Coefficient
AKT1	142	1.197740113	0.033697822	0.83490566	0.373589052
TNF	138	1.220338983	0.031741543	0.819444444	0.375330583
IL6	132	1.254237288	0.026524012	0.797297297	0.3901226
STAT3	128	1.282485876	0.021246143	0.779735683	0.416215551
SRC	128	1.276836158	0.031061707	0.783185841	0.406988189
TP53	127	1.282485876	0.023408794	0.779735683	0.420572428
JUN	126	1.288135593	0.023064671	0.776315789	0.417904762
MAPK3	120	1.322033898	0.020543412	0.756410256	0.425770308
EGFR	120	1.322033898	0.018283589	0.756410256	0.430952381
HRAS	119	1.327683616	0.016924558	0.753191489	0.44651759

Table 6 Target Gene Protein Pocket Coordinates and Grid Box Sizes

PDB ID	Protein Pocket Coordinates	Grid Box Size
5JHB	X=33.217, Y=−19.873, Z=27.266	X=40, Y=40, Z=40
4Y6O	X=16.404, Y=23.931, Z=94.078	X=40, Y=40, Z=40
1ALU	X=2.523, Y=−19.96, Z=8.684	X=40, Y=40, Z=40
1UNQ	X=21.578, Y=−14.614, Z=9.955	X=40, Y=40, Z=40
7NG7	X=−12.135, Y=0.341, Z=−14.351	X=40, Y=40, Z=40
2VUK	X=114.500, Y=87.421, Z=−29.843	X=40, Y=40, Z=40
6NJS	X=−2.065, Y=19.922, Z=24.187	X=40, Y=40, Z=40

values than the model group ($P < 0.001$). Based on HE, PAS, and Masson staining analyses (Figure 4c–e), the lung tissues of mice in the model group showed marked inflammatory cell infiltration, goblet cell hyperplasia, a large amount of mucus secretion, and considerable collagen deposition. GMK-treated mice showed reduced numbers of inflammatory cells in the lung tissue, decreased goblet cell metaplasia, and improved collagen deposition.

The PI3K/Akt signaling pathway is known to play a key role in AA.[8,27] The pathway enrichment and molecular docking analyses revealed that the PI3K signaling pathway mediates the therapeutic effects of GMK in AA. The results

Table 7 Affinity Value (kcal/Mol) of the Groups of Main Ligands With Receptors (n = 70)

PubChem CID	Compound Name	5JHB	4Y6O	1ALU	1UNQ	7NG7	2VUK	6NJS
21633085	Methyl lucidenate F	−9.561	−8.454	−6.514	−6.751	−8.516	−8.699	−7.446
11271456	Methyl lucidenate Q	−9.009	−8.248	−6.612	−6.352	−7.426	−7.849	−7.744
21,635,716	15alpha,26-Dihydroxy-5alpha-lanosta-7,9(11),24-triene-3-one	−9.587	−8.05	−6.279	−6.533	−7.319	−7.861	−7.9
73400	Dauricine	−9.508	−8.948	−6.066	−6.993	−8.693	−8.435	−8.379
442126	Decursin	−8.387	−7.823	−7.113	−7.146	−8.607	−7.303	−7.463
14015434	Epoxyganoderiol A	−9.303	−8.546	−7.589	−6.525	−8.143	−8.897	−7.649
21636089	Methyl lucidenate A	−9.279	−8.597	−6.367	−6.608	−6.962	−8.505	−7.71
132,113	3,7,12,23-Tetrahydroxy-26,28-epoxy-16,23-cyclolanost-8-ene-11,15,26-trione	−10.67	−9.522	−7.185	−7.325	−7.628	−8.321	−8.772
643684	Ricinoleic acid	−6.482	−4.63	−4.35	−4.799	−5.908	−4.657	−4.684
10212	Imperatorin	−8.642	−6.778	−6.335	−6.227	−7.925	−6.825	−6.583

of Western blot also indicated that GMK regulates the PI3K/Akt signaling pathway in the lung tissue of AA mice (Figure 4f and g). Compared with the model group, the GMK group exhibited significantly reduced levels of PI3K and AKT phosphorylation in the lung tissues ($P < 0.05$). These findings indicate that the PI3K/Akt signaling pathway was suppressed in the lung tissues of GMK-treated mice.

Bioinformatics Analysis of AA and the PI3K/Akt Pathway

After downloading the GSE104468 dataset from the GEO database, 388 DEGs (106 genes up-regulated and 282 down-regulated in AA patients) were screened using the Limma package ($P < 0.05$, $|\log FC| > 0.9$) (Figure 5a–d). Further GO enrichment analyses of BP, CC and MF showed its role in the positive regulation of phosphatidylinositol 3-kinase activity, T cell receptor signaling pathway and MHC class II receptor activity, KEGG pathway was enriched in Asthma, Antigen processing and presentation and Th1 and Th2 cell differentiation (Figure 5e and f). To further analyse the correlation of these asthma disease genes with the PI3K-Akt pathway, we downloaded the PI3K-Akt pathway genes included in the KEGG pathway, showing that nine genes overlapped, and the PPI network showed the links between them, using pie charts to represent the strength of the positive and negative correlations between these genes (Figure 5g–i).

Discussion

AA, an allergen-induced subtype of asthma, is characterized by eosinophilic airway inflammation, bronchial hyperreactivity, and elevated IgE levels, frequently combined with allergic rhinitis and conjunctivitis. AA has become a serious threat to human health. Our study used network pharmacology, molecular docking, bioinformatics and other experimental methods to analyze the key components and targets of GMK's therapeutic effect on AA, proving that the PI3K/Akt pathway may play an important role in the treatment of AA.

Previous studies have shown that numerous factors participate in the development of AA, with genetic inheritance, epigenetic inheritance, intestinal flora, and cellular immune balance all influencing the development of AA.[28] AA involves a variety of cells, including mast cells, eosinophils, and T lymphocytes. Th2 cells are classical helper T cells that contribute to the development of asthma and produce IL-4, IL-5, and IL-13, important cytokines in AA.[29,30] In response to transforming growth factor (TGF)-β and IL-4 cytokines, $CD4^+$ T cells can differentiate into a type of IL-9-secreting helper T lymphocyte, Th9, which is a growth and differentiation factor for mast cells and promotes inflammation by stimulating the secretion of chemokines that recruit other pro-inflammatory cells to the inflammatory site.[31,32] Th17 and Tregs are functionally antagonistic and act together to maintain immune homeostasis. Th17 cells secrete glucocorticoid-resistant IL-17A, IL-17F, and IL-22, cytokines capable of inducing neutrophilic airway inflammation, cupped cell hyperplasia, increased mucus secretion, and airway smooth muscle hyperplasia, thereby resulting in airway remodeling.[33,34]

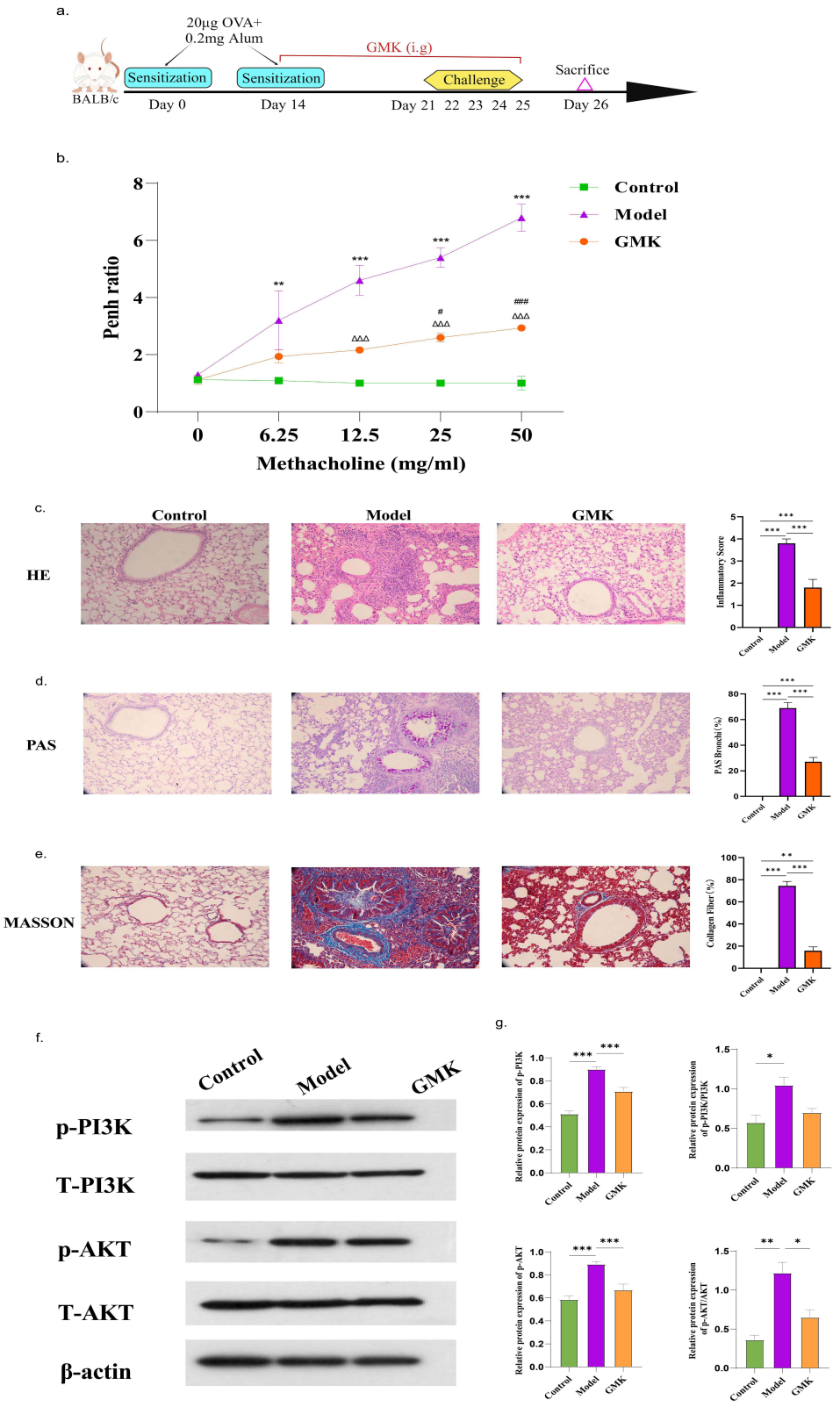

Figure 4 GMK treatment regulated inflammatory responses in OVA-induced mice. (**a**) Establishing a timeline of AA mouse model. (**b**) The Penh values of each group of mice were assessed using a non-invasive method (n=6, $^{**}P < 0.01$ vs Control group, $^{***}P < 0.001$ vs Control group, $^{\Delta\Delta\Delta}P < 0.001$ vs Model group, $^{\#}p < 0.05$ vs GMK group, $^{\#\#\#}p < 0.001$ vs GMK group). (c) HE staining and inflammation score of lung tissue (**d**) Typical PAS staining and percentage of positive cupped cells (**e**) Masson staining and collagen fibril deposition rate of lung tissue (×200 magnification) (**f** and **g**) Comparison of protein expression of p-PI3K and p-Akt in lung tissue of mice in each group (n=6, $^{*}P < 0.05$, $^{**}P < 0.01$, $^{***}P < 0.001$).

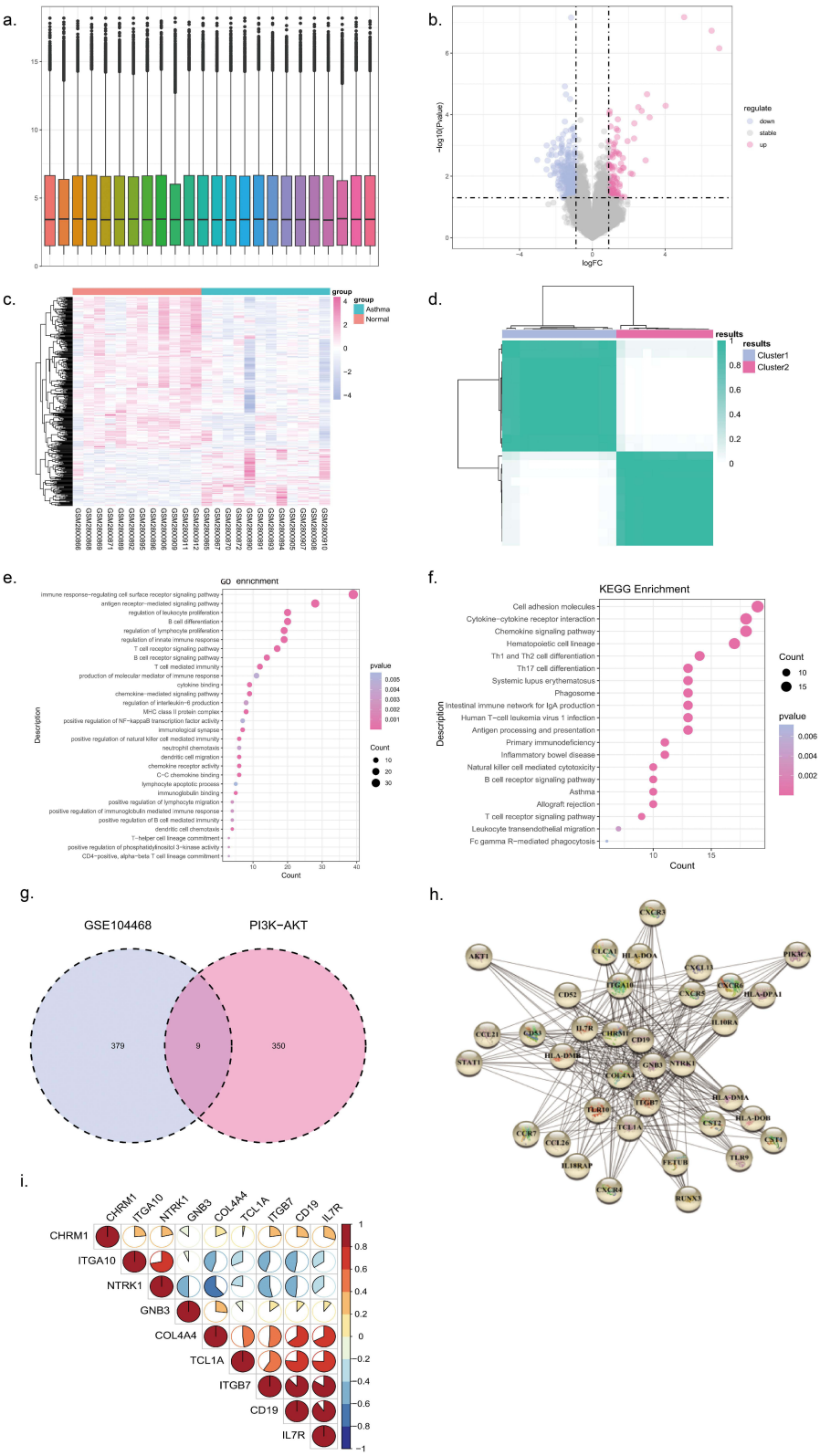

Figure 5 Bioinformatics analysis of data sets. (**a**) Box line blots of GSE104468 (**b**) Volcano map of DEGs (Up-regulated genes were labelled pink and down-regulated genes were labelled blue) (**c**) Heatmap of the significantly upregulated or downregulated DEGs (**d**) Heatmap of the matrix of co-occurrence information for AA samples (**e** and **f**) GO and KEGG analyses of DEGs between asthma group and healthy group (**g**) Venn diagram showing 9 overlapping genes associated with PI3K-AKT and DEGs (**h**) PPI of DEGs and overlapping genes (**i**) Correlation between 9 intersecting genes.

https://doi.org/10.2147/JIR.S484251

Currently, medications used to treat asthma are classified into two categories: control medications and reliever medications. However, the use of these medications is associated with a number of side effects.[35] Epidemiological surveys have revealed that asthma-related morbidity and mortality are increasing annually, and there is a lack of specific drugs for treating asthma in modern medicine, therefore, there is an urgent need to develop alternative therapeutic agents that can effectively control or treat asthma.[36] TCM has unique advantages in the treatment of allergic diseases. GMK is a traditional Chinese medicine compound formula composed of six Chinese medicines under the guidance of the diagnostic and therapeutic modes of constitution-disease differentiation, which has shown good efficacy in clinical practice, but its mechanism of action has been less studied. And the holistic nature of network pharmacology is well-suited to Chinese medicine research, with the help of databases and networks to analyze the interrelationships between drugs, targets, and diseases. Here, 267 active ingredients and 475 related genes of GMK were screened for compounds with potent biological activity and oral availability based on the principle of five classes of drugs. Among them, decursin derivatives have been found to considerably inhibit elevated leukocyte and eosinophil levels in the bronchoalveolar lavage fluid, decrease mucus secretion and IgE levels, and induce mucus hypersecretion.[37] Imperatorin reportedly exerts good expectorant, analgesic, and anti-inflammatory effects and has been shown to improve mast cell-mediated allergic airway inflammation by inhibiting the MRGPRX2 and CamKII/ERK signaling pathways.[38] Furthermore, imperatorin was shown to reduce IL-4, IL-5, and IL-13 production via Th2 cells, promote IFN-γ and IL-12 production via Th1 cells, and enhance IL-10 production in bronchoalveolar lavage fluid.[39] However, in the present study, molecular docking revealed that the most important active ingredient was 3,7,12,23-Tetrahydroxy-26,28-epoxy-16,23-cyclolanost-8-ene-11,15,26-trione (PubChem CID: 132113), 15alpha,26-Dihydroxy-5alpha-lanosta-7,9(11),24-triene-3-one (PubChem CID: 21635716), which is the first time that a compound has been identified that can act on the disease target of AA to exert therapeutic effects. Therefore, in future studies, we will continue to investigate the potential mechanisms by which multiple components of network pharmacology work together to treat AA.

We constructed a PPI network using common targets of GMK and AA and analyzed the main gene functions using GO and KEGG, then six targets were identified in the data mining process. Allergen-induced inflammation drives TNF-dependent innate memory, which may maintain and aggravate chronic type 2 airway inflammation, affording a potential target for asthma therapy.[40] IL-6, a key factor necessary for Th17 cell differentiation, interacts with TGF-β to promote Th17 cell differentiation and inhibit Treg proliferation, resulting in a Th17/Treg imbalance. In a mouse model of asthma, Src kinase mediates epidermal growth factor receptor transactivation, which, in turn, stimulates multiple downstream signaling pathways involving ERK1/2 and PI3Kδ, as well as the transcription factor NF-κB to regulate allergic lung inflammation, with SCR inhibition contributing to an improved phenotype of AA.[41] Inhibition of vascular endothelial growth factor (VEGF) was found to attenuate asthma symptoms in mice, and studies have analyzed polymorphisms in the VEGFA gene that may be associated with the response to asthma treatment.[42] Elevated levels of phosphorylated STAT3 or STAT3 deficiency reportedly ameliorate Th2-associated allergic lung inflammation.[43,44]

In addition, AKT1 is an important target that mediates the PIK3/Akt signaling pathway, while PI3K is a kinase that regulates tumor signaling pathways that affect and regulate inflammatory cells and inflammatory factors closely associated with the development of AA. Phenotypic regulation of AA through PI3K/Akt has been found in this network pharmacology studies. In asthma, PI3K regulates many inflammatory cytokines as well as neutrophil, eosinophil, and macrophage recruitment and activation, and in OVA-sensitized mice, accompanied by enhanced expression of PI3K pathway proteins, enhanced inflammatory cell infiltration and an IL-13 / IFN-γ cytokine imbalance were observed in lung tissue.[45] Targeting PI3K/Akt for the treatment of asthma has also been reported in previous studies. Inhibition of PI3K/AKT/mTOR signaling by targeted molecules attenuates asthma pathology and plays an important role in airway protection,[8] eg, the natural compound Bixin acts as a potent antagonist of PI3K/Akt signaling to prevent AA.[46] This target is therefore central to the treatment of asthma. Using a mouse model of AA, we showed that the PI3K/Akt signaling pathway was suppressed in the GMK-treated group, with mice exhibiting fewer symptoms of airway inflammation than the control group. We proceeded to verify the correlation between allergic asthma and the PI3K-Akt pathway using publicly available data from GEO, employing the R language statistical software. Overall, our findings suggest that PI3K/Akt plays a major role in mediating the effects of GMK against AA. However, the current study has several limitations. Firstly, the mechanisms by which the key active components of GMK modulate other

signaling pathways in AA were not investigated in this study. Secondly, in vitro experiments using cells to directly demonstrate the protective effects of GMK on the airway were not performed.

Conclusions

The objective of this study was to elucidate the mechanisms by which GMK exerts its therapeutic effects on AA. To achieve this goal, network pharmacological methods, bioinformatics analyses, and animal experiments were employed. The results demonstrated that the PI3K/AKT signaling pathway plays a pivotal role in AA, and GMK exerts therapeutic effects by regulating the PI3K/AKT signaling pathway. This provides an experimental basis for the clinical application and further development of GMK.

Ethics Approval and Informed Consent

This use of the database does not require the consent of the owner. The databases on humans used in this paper are publicly available and allow for unrestricted re-use through an open licence. This study was approved by the Ethics Committee of Beijing University of Chinese Medicine. Permit numbers: BUCM-1-2020102701-0010.

Acknowledgments

The Project Supported by the Fundamental Research Funds for the Central Universities (No. 2023-JYB-JBZD-009, 2023-JYB-XJSJJ-016), the National Natural Science Foundation of China (No. 82174243, 82204948), General project of Beijing Natural Science Foundation (No. 7242227), and High level Key Discipline of National Administration of Traditional Chinese Medicine - Traditional Chinese constitutional medicine (No. zyyzdxk-2023251).

Author Contributions

All authors made a significant contribution to the work reported, whether that is in the conception, study design, execution, acquisition of data, analysis and interpretation, or in all these areas; took part in drafting, revising or critically reviewing the article; gave final approval of the version to be published; have agreed on the journal to which the article has been submitted; and agree to be accountable for all aspects of the work.

Disclosure

The authors declare that they have no known competing financial interests or personal relationships that could have appeared to influence the work reported in this paper.

References

1. Bateman ED, Hurd SS, Barnes PJ, et al. Global strategy for asthma management and prevention: GINA executive summary. *Eur Respir J*. 2008;31(1):143–178. doi:10.1183/09031936.00138707
2. Morales E. The Global Asthma Report 2018. 2018.
3. Barakat L, Torres MJ, Phillips EJ, et al. Biological treatments in allergy: prescribing patterns and management of hypersensitivity reactions. *J Allergy Clin Immunol Pract*. 2021;9(3):1396–1399.e2. doi:10.1016/j.jaip.2020.10.044
4. Ebina-Shibuya R, Leonard WJ. Role of thymic stromal lymphopoietin in allergy and beyond. *Nat Rev Immunol*. 2022;22:1–14. doi:10.1038/s41577-022-00735-y
5. Lommatzsch M, Buhl R, Korn S. The treatment of mild and moderate asthma in adults. *Dtsch Arztebl Int*. 2020;117(25):434–444. doi:10.3238/arztebl.2020.0434
6. Sun P, Liu X, Wang Y, et al. Molecular characterization of allergic constitution based on network pharmacology and multi-omics analysis methods. *Medicine*. 2024;103(7):e36892. doi:10.1097/md.0000000000036892
7. Zhou Y, Hu L, Zhang H, et al. Guominkang formula alleviate inflammation in eosinophilic asthma by regulating immune balance of Th1/2 and Treg/Th17 cells. *Front Pharmacol*. 2022;13:978421. doi:10.3389/fphar.2022.978421
8. Ma B, Athari SS, Mehrabi Nasab E, Zhao L. PI3K/AKT/mTOR and TLR4/MyD88/NF-κB signaling inhibitors attenuate pathological mechanisms of allergic asthma. *Inflammation*. 2021;44(5):1895–1907. doi:10.1007/s10753-021-01466-3
9. Huang P, Li Y, Lv Z, et al. Comprehensive attenuation of IL-25-induced airway hyperresponsiveness, inflammation and remodelling by the PI3K inhibitor LY294002. *Respirology*. 2017;22(1):78–85. doi:10.1111/resp.12880
10. Tirpude NV, Sharma A, Joshi R, Kumari M, Acharya V. Vitex negundo Linn. extract alleviates inflammatory aggravation and lung injury by modulating AMPK/PI3K/Akt/p38-NF-κB and TGF-β/Smad/Bcl2/caspase/LC3 cascade and macrophages activation in murine model of OVA-LPS induced allergic asthma. *J Ethnopharmacol*. 2021;271:113894. doi:10.1016/j.jep.2021.113894

11. Yan X, Tong X, Jia Y, et al. Baiheqingjin formula reduces inflammation in mice with asthma by inhibiting the PI3K/AKT/NF-κb signaling pathway. *J Ethnopharmacol*. 2024;321:117565. doi:10.1016/j.jep.2023.117565
12. Smyth GK. Linear models and empirical Bayes methods for assessing differential expression in microarray experiments. *Stat Appl Genet Mol Biol*. 2004;3:Article3. doi:10.2202/1544-6115.1027
13. Ru J, Li P, Wang J, et al. TCMSP: a database of systems pharmacology for drug discovery from herbal medicines. *J Cheminform*. 2014;6:13. doi:10.1186/1758-2946-6-13
14. Fang S, Dong L, Liu L, et al. HERB: a high-throughput experiment- and reference-guided database of traditional Chinese medicine. *Nucleic Acids Res*. 2021;49(D1):D1197–D1206. doi:10.1093/nar/gkaa1063
15. Kim S, Chen J, Cheng T, et al. PubChem in 2021: new data content and improved web interfaces. *Nucleic Acids Res*. 2021;49(D1):D1388–D1395. doi:10.1093/nar/gkaa971
16. Daina A, Michielin O, Zoete V. SwissADME: a free web tool to evaluate pharmacokinetics, drug-likeness and medicinal chemistry friendliness of small molecules. *Sci Rep*. 2017;7:42717. doi:10.1038/srep42717
17. Daina A, Michielin O, Zoete V. SwissTargetPrediction: updated data and new features for efficient prediction of protein targets of small molecules. *Nucleic Acids Res*. 2019;47(W1):W357–W364. doi:10.1093/nar/gkz382
18. UniProt C, Martin M-J, Orchard S. UniProt: the universal protein knowledgebase in 2021. *Nucleic Acids Res*. 2021;49(D1):D480–D489. doi:10.1093/nar/gkaa1100
19. Amberger JS, Bocchini CA, Schiettecatte F, Scott AF, Hamosh A. OMIM.org: online Mendelian Inheritance in Man (OMIM(R)), an online catalog of human genes and genetic disorders. *Nucleic Acids Res*. 2015;43(Database issue):D789–98. doi:10.1093/nar/gku1205
20. Pinero J, Sauch J, Sanz F, Furlong LI. The DisGeNET Cytoscape app: exploring and visualizing disease genomics data. *Comput Struct Biotechnol J*. 2021;19:2960–2967. doi:10.1016/j.csbj.2021.05.015
21. Stelzer G, Rosen N, Plaschkes I, et al. The genecards suite: from gene data mining to disease genome sequence analyses. *Curr Protoc Bioinformatics*. 2016;54(1):301–13033. doi:10.1002/cpbi.5
22. Wishart DS, Feunang YD, Guo AC, et al. DrugBank 5.0: a major update to the DrugBank database for 2018. *Nucleic Acids Res*. 2018;46(D1):D1074–D1082. doi:10.1093/nar/gkx1037
23. Shannon P, Markiel A, Ozier O, et al. Cytoscape: a software environment for integrated models of biomolecular interaction networks. *Genome Res*. 2003;13(11):2498–2504. doi:10.1101/gr.1239303
24. Szklarczyk D, Gable AL, Nastou KC, et al. The STRING database in 2021: customizable protein-protein networks, and functional characterization of user-uploaded gene/measurement sets. *Nucleic Acids Res*. 2021;49(D1):D605–D612. doi:10.1093/nar/gkaa1074
25. Ma H, He Z, Chen J, Zhang X, Song P. Identifying of biomarkers associated with gastric cancer based on 11 topological analysis methods of CytoHubba. *Sci Rep*. 2021;11(1):1331. doi:10.1038/s41598-020-79235-9
26. Tang Y, Li M, Wang J, Pan Y, Wu FX. CytoNCA: a Cytoscape plugin for centrality analysis and evaluation of protein interaction networks. *Biosystems*. 2015;127:67–72. doi:10.1016/j.biosystems.2014.11.005
27. Zhao Y, Li X, Xu Z, Hao L, Zhang Y, Liu Z. PI3K-AKT-mTOR signaling pathway: the intersection of allergic asthma and cataract. *Pharmazie*. 2019;74(10):598–600. doi:10.1691/ph.2019.9080
28. Wang J, Zhou Y, Zhang H, et al. Pathogenesis of allergic diseases and implications for therapeutic interventions. *Signal Transduct Target Ther*. 2023;8(1):138. doi:10.1038/s41392-023-01344-4
29. Akar-Ghibril N, Casale T, Custovic A, Phipatanakul W. Allergic endotypes and phenotypes of asthma. *J Allergy Clin Immunol Pract*. 2020;8(2):429–440. doi:10.1016/j.jaip.2019.11.008
30. León B, Ballesteros-Tato A. Modulating Th2 cell immunity for the treatment of asthma. *Front Immunol*. 2021;12:637948. doi:10.3389/fimmu.2021.637948
31. Koch S, Sopel N, Finotto S. Th9 and other IL-9-producing cells in allergic asthma. *Semin Immunopathol*. 2017;39(1):55–68. doi:10.1007/s00281-016-0601-1
32. Übel C, Graser A, Koch S, et al. Role of Tyk-2 in Th9 and Th17 cells in allergic asthma. *Sci Rep*. 2014;4:5865. doi:10.1038/srep05865
33. Chen X, Yue R, Li X, Ye W, Gu W, Guo X. Surfactant protein A modulates the activities of the JAK/STAT pathway in suppressing Th1 and Th17 polarization in murine OVA-induced allergic asthma. *Lab Invest*. 2021;101(9):1176–1185. doi:10.1038/s41374-021-00618-1
34. Gregorczyk I, Jasiecka-Mikołajczyk A, Maślanka T. Blockade of NF-κB Translocation and of RANKL/RANK interaction decreases the frequency of Th2 and Th17 cells capable of IL-4 and IL-17 production, respectively, in a mouse model of allergic asthma. *Molecules*. 2021;26(11):3117. doi:10.3390/molecules26113117
35. Papadopoulos NG, Miligkos M, Xepapadaki P. A current perspective of allergic asthma: from mechanisms to management. In: Traidl-Hoffmann C, Zuberbier T, Werfel T, editors. *Allergic Diseases – From Basic Mechanisms to Comprehensive Management and Prevention*. Springer International Publishing; 2022:69–93.
36. Papi A, Brightling C, Pedersen SE, Reddel HK. Asthma. *Lancet*. 2018;391(10122):783–800. doi:10.1016/s0140-6736(17)33311-1
37. Yang EJ, Song GY, Lee JS, Yun CY, Kim IS. A novel (S)-(+)-decursin derivative, (S)-(+)-3-(3,4-dihydroxy-phenyl)-acrylic acid 2,2-dimethyl-8-oxo-3,4-dihydro-2H,8H-pyrano[3,2-g]chromen-3-yl-ester, inhibits ovalbumin-induced lung inflammation in a mouse model of asthma. *Biol Pharm Bull*. 2009;32(3):444–449. doi:10.1248/bpb.32.444
38. Wang N, Wang J, Zhang Y, et al. Imperatorin ameliorates mast cell-mediated allergic airway inflammation by inhibiting MRGPRX2 and CamKII/ERK signaling pathway. *Biochem Pharmacol*. 2021;184:114401. doi:10.1016/j.bcp.2020.114401
39. Hsieh CC, Ng YY, Li WS, et al. Ameliorative effect of imperatorin on Dermatophagoides pteronyssinus-induced allergic asthma by suppressing the Th2 response in mice. *Molecules*. 2022;27(20):7028. doi:10.3390/molecules27207028
40. Lechner A, Henkel FDR, Hartung F, et al. Macrophages acquire a TNF-dependent inflammatory memory in allergic asthma. *J Allergy Clin Immunol*. 2022;149(6):2078–2090. doi:10.1016/j.jaci.2021.11.026
41. El-Hashim AZ, Khajah MA, Renno WM, et al. Src-dependent EGFR transactivation regulates lung inflammation via downstream signaling involving ERK1/2, PI3Kδ/Akt and NFκB induction in a murine asthma model. *Sci Rep*. 2017;7(1):9919. doi:10.1038/s41598-017-09349-0
42. Balantic M, Rijavec M, Skerbinjek Kavalar M, et al. Asthma treatment outcome in children is associated with vascular endothelial growth factor A (VEGFA) polymorphisms. *Mol Diagn Ther*. 2012;16(3):173–180. doi:10.1007/bf03262206

43. Lu D, Lu J, Ji X, et al. IL-27 suppresses airway inflammation, hyperresponsiveness and remodeling via the STAT1 and STAT3 pathways in mice with allergic asthma. *Int J Mol Med*. 2020;46(2):641–652. doi:10.3892/ijmm.2020.4622
44. Fu L, Zhao J, Huang J, et al. A mitochondrial STAT3-methionine metabolism axis promotes ILC2-driven allergic lung inflammation. *J Allergy Clin Immunol*. 2022;149(6):2091–2104. doi:10.1016/j.jaci.2021.12.783
45. Jiang X, Fang L, Wu H, et al. TLR2 regulates allergic airway inflammation and autophagy through PI3K/Akt signaling pathway. *Inflammation*. 2017;40(4):1382–1392. doi:10.1007/s10753-017-0581-x
46. Zhu Y, Sun D, Liu H, et al. Bixin protects mice against bronchial asthma though modulating PI3K/Akt pathway. *Int Immunopharmacol*. 2021;101 (Pt B):108266. doi:10.1016/j.intimp.2021.108266